

# Fisheye stereo camera using equirectangular images

Akira Ohashi, Yuki Tanaka  
Gakuto Masuyama and Kazunori Umeda  
Chuo University  
Tokyo, Japan  
Email: ohashi@sensor.mech.chuo-u.ac.jp

Daisuke Fukuda, Takehito Ogata  
Tatsuro Narita, Shuzo Kaneko  
and Yoshitaka Uchida  
Clarion  
Saitama, Japan

Kota Irie  
Hitachi Automotive Systems Americas  
Farmington Hills, USA

**Abstract**—This paper proposes making a stereo camera using two fisheye cameras. The measurement range of the stereo camera is increased by using fisheye cameras. Fisheye images are deformed by using an equirectangular projection to simplify the stereo correspondence search in the images. Perspective transformation is applied to images so that feature points of far objects coincide in the images of the two cameras in order to remove mismatches due to the errors of intrinsic and extrinsic parameters. The corresponding points are calculated by using stereo matching in the deformed image, and the distance is measured from the disparity. The accuracy of the constructed stereo camera's distance measuring is evaluated by experiments. The performance of the constructed stereo camera is evaluated by indoor and outdoor experiments.

## I. INTRODUCTION

In recent years, the installation of a camera and a three-dimensional measurement sensor for driving assistance is increasing in vehicles. Since the cost is proportional to the quantity of the sensor, the sensor should capture a wide range of environmental information. In this paper, we focus on a fisheye camera. The fisheye camera has a view angle of 180 degrees or more, and its size is relatively small. Therefore, the fisheye camera is easily installed in a vehicle or robot. Several studies have been carried out to use fisheye cameras for vehicles, such as lane detection [1], estimation of vehicle pose [2], and obstacle detection [3]. In some studies, a driver assistance system is constructed using multiple fisheye cameras [4] [5]. An overhead view of the entire circumference is created from the multiple camera images.

By using two fisheye cameras, a fisheye stereo camera can be constructed. Abraham and Forstner [6] simplified stereo matching by rectifying the images of the fisheye stereo camera. Moreau *et al.* [7] discussed the epipolar constraint of fisheye image for equisolid angle projection model and achieved environment restoration using a stereo camera. However, the method requires large computational cost. Hane *et al.* [8] achieved real-time three-dimensional measurement by using the plane-sweeping method. In some studies, a fisheye stereo camera was applied to a practical platform such as UAV [9] and vehicles [10] [11] [12]. In these studies, fisheye images are usually transformed to perspective images in order to simplify the corresponding point search of stereo images. With this, the peripheral regions of the image are stretched strongly. Consequently, it becomes difficult to carry out stereo matching

at the peripheral regions and the detection range of the distance becomes narrower than using original fisheye images.

In this paper, we propose an equirectangular projection as a method to solve this problem. Equirectangular projection transforms the image to the planar rectangular coordinate system whose vertical axis and the horizontal axis are the latitude and the longitude, respectively. This projection method can simplify the corresponding point search without stretching the peripheral regions strongly. One drawback of this projection is that it stretches the regions closer to the upper and lower poles of the hemisphere of the fisheye. However, it is not a problem for many applications such as a vehicle sensor, because vertical angle about 130 degrees is sufficient for viewing the ground and the horizontal line. We show that easy and accurate stereo matching is achieved in the entire image by applying equirectangular projection on the fisheye stereo camera. To do this, we construct a fisheye stereo camera and verify the effectiveness of the proposed method by experiments using the camera in both indoor and outdoor environments.

## II. FISHEYE CAMERA OVERVIEW

### A. Fisheye Camera Model

There are several projection models of a fisheye lens, for example, an equidistant projection model, an orthogonal projection, a stereographic projection and an equisolid angle projection. These models define the relation between the distance from the center of the image to a point in an image and an angle from the optical axis to the point. However, an actual fisheye camera does not follow exactly such an ideal projection model. In this paper, we calculate the intrinsic parameters using a camera model proposed by Scaramuzza *et al.* [13]. An outline of the camera model is shown in Fig. 1. The correspondence between a three-dimensional vector  $\mathbf{P} = [X \ Y \ Z]^T$  and the image coordinates  $\mathbf{p} = [u \ v]^T$  is expressed as

$$\mathbf{P} = \begin{bmatrix} X \\ Y \\ Z \end{bmatrix} \approx \begin{bmatrix} u - u_0 \\ v - v_0 \\ f(\rho) \end{bmatrix}, \quad (1)$$

where  $\approx$  indicates equal homogeneous coordinates. Here,  $\rho = \sqrt{(u - u_0)^2 + (v - v_0)^2}$  is the distance from the image center

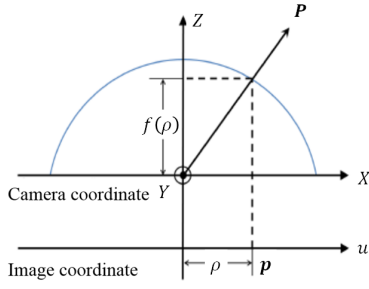
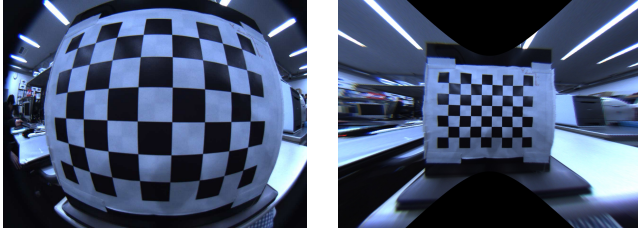


Fig. 1. Fisheye camera model to be used in the intrinsic parameter estimation [13]



(a) Fisheye image (b) Perspective image

Fig. 2. Stretching by the perspective projection

of  $\mathbf{p}_0 = [u_0 \ v_0]^T$  of image coordinates  $\mathbf{p} = [u \ v]^T$ .  $f(\rho)$  is the polynomial equation of  $\rho$ , and it is expressed as

$$f(\rho) = a_0 + a_1\rho + a_2\rho^2 + a_3\rho^3 + a_4\rho^4 + \dots \quad (2)$$

In this paper, we regard the intrinsic parameters of the camera as the coefficient up to quartic  $a_0, a_1, a_2, a_3, a_4$ . As explained above, the intrinsic parameters of the camera  $\mathbf{I}$  are expressed as

$$\mathbf{I} = [a_0 \ a_1 \ a_2 \ a_3 \ a_4 \ u_0 \ v_0]^T. \quad (3)$$

### B. Cylindrical Projection Model

Characteristic distortion is a problem when using a fisheye image. Since this distortion greatly influences the search for stereo correspondence, a fisheye camera cannot apply the same method of stereo matching as do normal stereo cameras. In general, the distortion of a fisheye image is removed by using a perspective projection before processing the image. The same image processing method that is used for normal cameras can be applied to fisheye images when a perspective projection has been applied. However, as shown in Fig. 2, when perspective projection is applied to a fisheye image, the center of the image is shrunk, and the periphery of the image is stretched. As an example, Fig. 2(a) is taken by a fisheye camera with 180 degrees of the angle of view; although an image sensor is small in contrast with a fisheye lens, some area of the fisheye image is lacking. Fig. 2(b) shows the result of a perspective projection to Fig. 2(a), and its field of view is 156 degrees in the horizontal and 123 degrees in the vertical. When some area of the image is reduced or stretched, that area cannot be used to search for a stereo correspondence. In other words, the accuracy of the distance

information is deteriorated. Equirectangular projection is a projection system whose vertical axis of the rectangular plane applies the longitude in the hemisphere of a fisheye, and the horizontal axis of a rectangular plane applies the latitude in the hemisphere of a fisheye. Therefore, to remove the distortion of the fisheye image and decrease the stretching of image by projection, equirectangular projection is applied to the fisheye image. Since equirectangular projection can change the fisheye image into an image vertically equidistant, which is low distortion, and keep the form of the image, the images with equirectangular projection can easily search for stereo correspondence. The process of the equirectangular projection is described below.

#### (a) Selection of a pixel of the equirectangular image

The image generated by the equirectangular projection (called an equirectangular image in this paper) is shown in Fig. 3(a). The number of pixels in an equirectangular image is  $M \times N$ . The equirectangular image is created by inserting the pixel value of the fisheye image into the target pixel position of the equirectangular image  $\mathbf{p}' = [u' \ v']^T$ .

#### (b) Projection to the cylindrical model

The target pixel position of an equirectangular image projects a cylindrical model, which is shown in Fig. 3(b). The vertical axis of a cylindrical model's rectangular plane applies an azimuth angle from the center of the hemisphere of fisheye  $\lambda$ , and a horizontal axis of a rectangular plane applies an elevation angle from the center of the hemisphere of a fisheye  $\phi$ . Furthermore, the  $M$  corresponds to  $\pi$  in this model, and the aspect ratio is 1:1. In this case, the correspondence between the target pixel position of the equirectangular image  $\mathbf{p}'$  and the target pixel position projected to the cylindrical model  $\mathbf{q}' = [\lambda, \phi]^T$  is expressed as

$$\lambda = \frac{\pi}{M} \left( u' - \frac{M}{2} \right), \quad (4)$$

$$\phi = -\frac{\pi}{M} \left( v' - \frac{N}{2} \right). \quad (5)$$

#### (c) Conversion to the polar coordinates

The target pixel position projected to the cylindrical model causes polar conversion, as shown in Fig. 3(c). The polar coordinate is the coordinates whose variables are the angle between the vector  $\mathbf{q}$  and  $Z$ -axis  $\theta$  and the azimuth angle from the center of the hemisphere of the fisheye  $\alpha$ . In this case, the correspondence between the target pixel position projected to the cylindrical model  $\mathbf{q}'$  and the target pixel position converted to polar conversion  $\mathbf{q} = [\theta, \alpha]^T$  is expressed as

$$\theta = \cos^{-1}(\cos \phi \cos \lambda), \quad (6)$$

$$\alpha = \tan^{-1} \frac{\tan \phi}{\sin \lambda}. \quad (7)$$

#### (d) Projection to the fisheye image

The target pixel position converted to polar conversion projects the fisheye image shown in Fig. 3(d) and obtain the pixel value of the fisheye image. In this case, the correspondence between the target pixel position's polar conversion  $\mathbf{q}'$

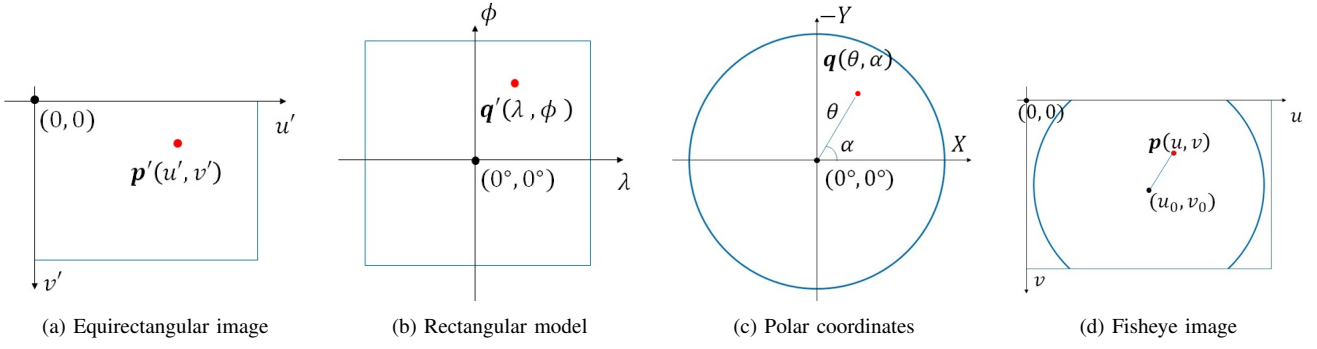


Fig. 3. Process of making equirectangular image

and the target pixel position of the fisheye image  $\mathbf{p} = [u, v]^T$  is expressed as

$$u = \rho \cos \alpha + u_0 = \rho \frac{\sin \lambda}{\sqrt{\tan^2 \phi + \sin^2 \lambda}} + u_0, \quad (8)$$

$$v = \rho \sin \alpha + v_0 = \rho \frac{\tan \phi}{\sqrt{\tan^2 \phi + \sin^2 \lambda}} + v_0. \quad (9)$$

$\rho$  is obtained by finding the real solutions of the quartic equation shown in (10) by using the intrinsic parameters.

$$a_0 + (a_1 + \frac{1}{\tan \theta})\rho + a_2\rho^2 + a_3\rho^3 + a_4\rho^4 = 0 \quad (10)$$

The equirectangular image is created by repeating the process of (a) ~ (d).

### III. DISTANCE MEASUREMENT

In this paper, three-dimensional measurement is implemented by applying the proposed method to the fisheye stereo camera. This section describes stereo image correction, a method for searching for corresponding points, and a method for calculating distance.

#### A. Alignment of the Image by the Perspective Transformation

The correspondence between the right and left images of an equirectangular image is inconsistent because of an error in the intrinsic parameter estimation and differences in the extrinsic parameters. To correct this discrepancy, the images are aligned by projective transformation, which is carried out by the following process.

##### (a) Extracting feature points at infinity

Feature points at infinity are extracted from the equirectangular image, which reflects a far target. Moreover, corresponding points are obtained from feature points at infinity. Feature points are extracted, and matching is performed using the AKAZE feature [14] [15]. Furthermore, it is difficult to capture an image that reflects the feature points at infinity in all areas with just one shot because a fisheye camera has very large angle of view. Therefore, many images are taken while rotating the camera, and feature points at infinity are obtained from the entire equirectangular image.

##### (b) Removal of the mismatch of corresponding points

Since the angle of view of the fisheye camera is extremely

large, it is difficult to take an image that is without near objects. Therefore, as shown in Fig. 4, near feature points are removed by selecting points manually.

##### (c) Calculation of parameters by corresponding points

When a camera takes feature points at infinity, the disparity between points in the left and right images is zero. Therefore, projective transformation to match feature points obtained at infinity can cancel the influence of errors of intrinsic parameter estimation and differences of extrinsic parameters. Furthermore, to improve the accuracy, outliers are removed by RANSAC, and inaccurate correspondence points are removed by the least-squares method.

#### B. Stereo Matching in Equirectangular Images

Epipolar lines of the image by perspective projection are horizontal straight. On the other hand, epipolar lines of the equirectangular image are curved. When the elevation angle of an azimuth angle of 0 is  $\phi_0$ , epipolar lines of equirectangular image can be expressed as

$$\phi = \tan^{-1}(\tan \phi_0 \cos \lambda). \quad (11)$$

Epipolar lines for some elevation angles are shown in Fig. 5.

#### C. Distance Measurement using an Equirectangular Image

The disparity of the equirectangular image is in inverse proportion to the cosine of an azimuth angle and in proportion to a cosine of an elevation angle. If the baseline length is  $b$ , the focal length is  $f$ , the pixel size is  $S$ , and the disparity of



Fig. 4. Extraction limiting and matching feature points at infinity

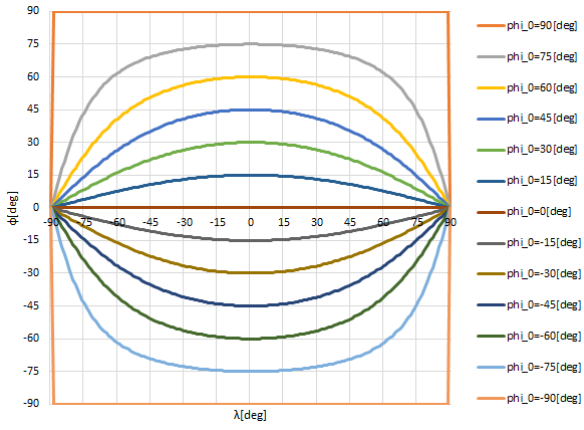


Fig. 5. Epipolar lines in an equirectangular image

the horizontal direction is  $\Delta u$ , the Euclidean distance between the camera and the object,  $D$ , is expressed as

$$D = \frac{bf \cos \lambda}{S \Delta u \cos \phi}. \quad (12)$$

From (12), we see that with the stereo camera, the measurement accuracy in the horizontal direction is better when the cameras are placed side by side vertically than when the cameras are placed side by side horizontally. However, installing cameras side by side vertically is difficult in vehicles. Therefore, for this paper, we placed cameras side by side horizontally.

#### IV. EXPERIMENTS

##### A. Experimental Conditions

The appearance of the fisheye stereo camera that was constructed is shown in Fig. 6. The CMOS camera that we used was the Point Grey Research Flea3.; the fisheye lens we used was the SPACE TV1634M. The number of pixels was  $1328 \times 1048$  [pixel]; the pixel size was  $3.63 \mu\text{m}$ ; the focal length of the lens was  $1.6 \text{ [mm]}$ ; the baseline length was  $52 \text{ [mm]}$ . The measurement range in the horizontal direction was  $165 \text{ [}^\circ\text{]}$ ; the vertical direction was  $132 \text{ [}^\circ\text{]}$ . Since it searches for corresponding points to the right during stereo matching, the measurement range in the horizontal direction is narrower than the horizontal angle of the camera's view. Intrinsic parameters of the fisheye camera were estimated by utilizing the OcamCalib Toolbox [13] in Matlab. The results of intrinsic parameter estimation are shown in Table 1. Moreover, reprojection errors of intrinsic parameters were calculated as shown in Fig. 7. Figure 7 shows reprojection errors that measured 200 sheets of the chess board that has  $7 \times 5$  corner points. The standard deviations  $\sigma_x$  and  $\sigma_y$  are  $0.8 \text{ [pixel]}$  and  $0.8 \text{ [pixel]}$  respectively. It is shown that reprojection errors are small and calibration of intrinsic parameters is successful. Using template matching in a search for corresponding points, SAD evaluation of similarity was used. Furthermore, the disparity is calculated in sub-pixel accuracy using equiangular linear fitting.

##### B. Comparison of Perspective and Equirectangular Projection

Fisheye images that are obtained by the constructed fisheye stereo camera are converted to the equirectangular images, and then disparity images and range images are constructed from them. First, we show an example of the constructed disparity image and range image, and compare the proposed equirectangular projection and the standard perspective projection. Perspective images are also converted from the fisheye images. The field of view was set to  $156 \text{ degrees}$  horizontally by  $123 \text{ degrees}$  vertically. Figure 8 shows the fisheye images of left and right cameras, and Fig. 9 and Fig. 10 show the converted perspective and equirectangular images respectively. Fig. 12(a) and Fig. 13(a) show the disparity images that were created from the left and right images of Fig. 9 and Fig. 10 respectively. The color of the red and blue corresponds to the magnitude of the disparity in Fig. 12(a) and Fig. 13(a), while Fig. 11(b) and Fig. 12(b) show range images that were created by applying equation (12) to Fig. 12(a) and Fig. 13(b). In Fig. 12(b) and Fig. 13(b), the color red indicates  $0.51 \text{ [m]}$ , and blue indicates  $10.00 \text{ [m]}$ . As shown in Fig. 12 and Fig. 13. As shown in Fig. 12 and Fig. 13, although some mismatching occurred, we found that the fisheye stereo camera can measure densely in all measurement ranges. The mismatching occurred with uneven brightness near the fluorescent lamp. It is assumed that the cause of mismatching is flatness of the displacement of the SAD score at the fluorescent lamps and the end of the image. Because it is impossible to avoid mismatching, it is necessary to remove the area that has high possibility of mismatching.

The number of matched points in the disparity images are  $134,670$  in the perspective image Fig. 11, and  $188,997$  in the equirectangular image Fig. 12 respectively. That is, the number of the matched points can be increased by using the equirectangular images. And, comparing Fig. 11 and Fig. 12, the disparity image by the equirectangular images is more detailed especially in the center of the area. In addition, it can be seen that the matching rate is better than the edge of the the disparity image by the perspective images. To summarize, it can be said that the equirectangular projection is more suitable than the perspective projection to construct fisheye images.

##### C. Evaluation of Distance Measurement Accuracy

We performed distance measurement experiments to evaluate the accuracy of the constructed stereo camera with the proposed method. The measurement position for evaluating errors was in front of the fisheye stereo camera, left and right to  $75 \text{ [}^\circ\text{]}$ , up and down to  $60 \text{ [}^\circ\text{]}$ , and in the oblique direction, as shown in Fig. 13. Fig. 14 is the result that shows the RMS errors of the measured distance. It was calculated by the average of five measurements. Each measured distance was obtained by the average of 25 points around the target point. As shown in Fig. 14, the distance measurement error is within  $14 \%$  until  $5 \text{ [m]}$  in measured points. Since distance measurement errors occur in all measurement points to the same extent, it is assumed that the proposed method can measure the distance near the edge of the image. However,



Fig. 6. The appearance of the fisheye stereo camera

TABLE I  
INTRINSIC PARAMETER

	left camera	right camera
$a_0$	$-4.713 \times 10^2$	$-4.731 \times 10^2$
$a_1$	0.000	0.000
$a_2$	$1.143 \times 10^{-3}$	$1.059 \times 10^{-3}$
$a_3$	$-1.564 \times 10^{-6}$	$-1.282 \times 10^{-6}$
$a_4$	$2.027 \times 10^{-9}$	$1.752 \times 10^{-9}$
$u_0$	$6.679 \times 10^2$	$6.660 \times 10^2$
$v_0$	$5.357 \times 10^2$	$5.346 \times 10^2$

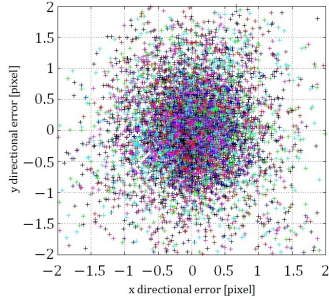


Fig. 7. Reprojection errors



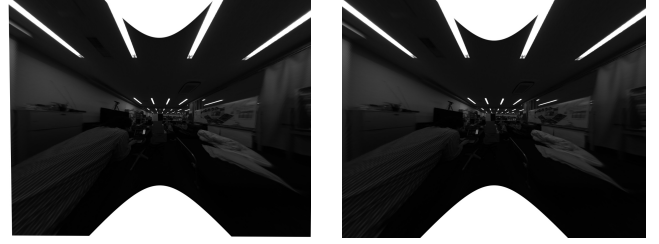
(a) Left image (b) Right image

Fig. 8. Fisheye images captured in the experimental environment

when comparing the ideal distance measurement error ( $\sigma$  of disparity: 0.2 pixel) shown in Fig. 15, with Fig. 14, it can be seen that distance measurement errors are not proportional to the distance or the measurement position. It is assumed that this is caused by the estimation error of the intrinsic parameters and extrinsic parameters or the location error of the measured target.

#### D. Outdoor experiments

We obtained range images in outdoor environments by the constructed fisheye stereo camera. Fig. 16 was obtained by tilting the fisheye stereo camera by 45 degrees. Fig. 16(b)



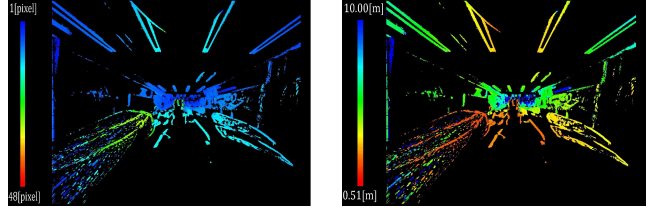
(a) Left image (b) Right image

Fig. 9. Perspective images converted from Fig. 8



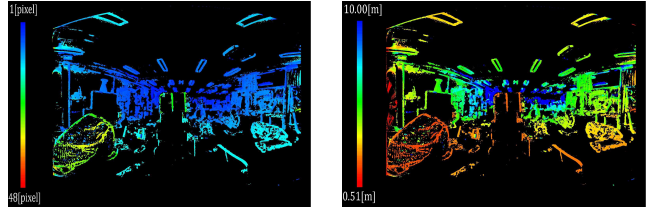
(a) Left image (b) Right image

Fig. 10. Equirectangular images converted from Fig. 8



(a) Disparity image (b) Range image

Fig. 11. Results of measurement using perspective images



(a) Disparity image (b) Range image

Fig. 12. Results of measurement using equirectangular images

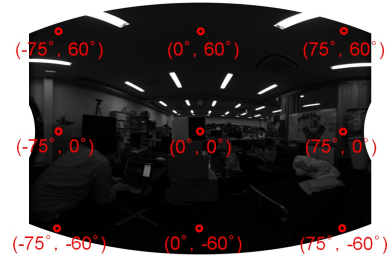


Fig. 13. The positions to measure distance

shows that the distances of vehicles at both sides and the pylon just below the camera are measured appropriately. In

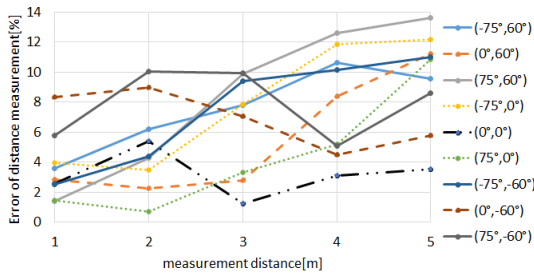


Fig. 14. The distance measurement error

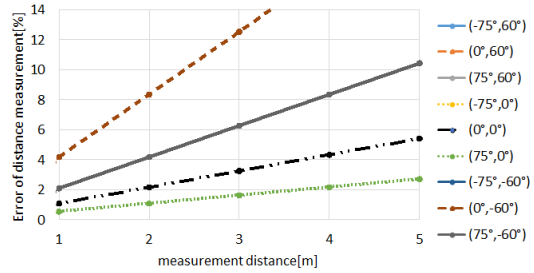


Fig. 15. The ideal error of the measured distance ( $\sigma$  of disparity: 0.2 pixel)

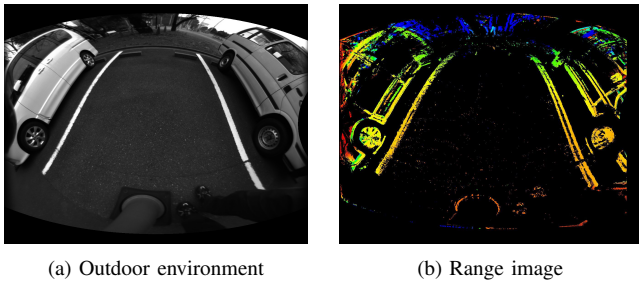


Fig. 16. The environment in which a pylon is under the fisheye stereo camera

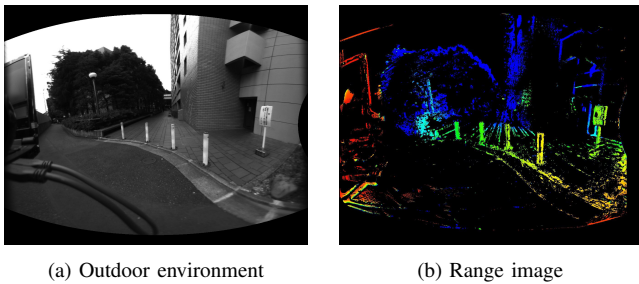


Fig. 17. The environment with far poles

addition, Fig. 17(b) shows that the fisheye stereo camera can measure both near and far objects, including the pole at the distance of 5 [m] (the farthest one). Note that the left object is a notebook PC and the cables that connect the camera and the PC. When we consider the sensors of the vehicles, sonars or laser sensors equipped with vehicles have issues that they cannot not observe the area under themselves, and that it is difficult to measure poles. The issues can be solved by the constructed fisheye stereo camera, which indicates that the camera is suitable for the usage of vehicles.

## V. CONCLUSIONS

In this paper, equirectangular projection was shown to be capable of converting fisheye images to equirectangular images that can extract feature points that are near the edges of an image. We proposed a three-dimensional measurement using equirectangular images. Our evaluation demonstrated the accuracy of the method for measuring distance, and it indicated that the proposed method can measure the distance densely.

We aim to improve the accuracy of distance measurement by improving the intrinsic and extrinsic parameter estimations.

## ACKNOWLEDGMENT

We thank ITAGAKIKINZOKU Corporation for the support of constructing the stereo camera.

## REFERENCES

- [1] C. H. Kum, D. C. Cho, M. S. Ra, and W. Y. Kim, Lane detection system with around view monitoring for intelligent vehicle, Proc. of SoC Design Conference (ISOCC), pp. 215-218, Busan, Korea, 2013.
- [2] S. Li, H. Oshima, and I. Nakanishi, Estimating vehicle pose relative to current lane from fisheye camera system, Trans. on the Institute of Electrical Engineers of Japan. C, A publication of Electronics, Information and Systems Society, vol. 131, no. 12, pp. 2189-2195, 2011.
- [3] C. T. Lin, Y. C. Lin, W. C. Liu, and C. W. Lin, A real-time rear obstacle detection system based on a fish-eye camera, Proc. of Signal Information Processing Association Annual Summit and Conference (APSIPA ASC), pp. 1-4, Hollywood, CA, USA, 2012.
- [4] T. Sato, A. Moro, A. Sugahara, T. Tasaki, A. Yamashita, and H. Asama, Spatio-temporal bird's-eye view images using multiple fish-eye cameras, Proc. of System Integration (SII), pp. 753-758, Kobe, Japan, December, 2013.
- [5] C. M. Huang, T. Y. Yang, K. Y. Lian, S. C. Chien, and M. F. Luo, Fish-eye cameras calibration for vehicle around view monitoring system, Proc. of Consumer Electronics - Taiwan (ICCE-TW), pp. 225-226, Taipei, Taiwan, 2014.
- [6] S. Abraham, W. Forstner, Fish-eye stereo calibration and epipolar rectification, Journal of Photogrammetry and Remote Sensing (ISPRS), 2005.
- [7] J. Moreau, S. Ambellouis and Y. Ruichek, Equisolid fisheye stereovision calibration and point cloud computation, Proc. of ISPRS - International Archives of the Photogrammetry, Remote Sensing and Spatial Information Sciences, Volume XL-7/W2, pp.167-172, 2013.
- [8] C. Hane, L. Heng, G. H. Lee, A. Sizov, M. Pollefeys, Real-time direct dense matching on fisheye images using plane-sweeping stereo, Proc. of Conference on 3D Vision (3DV), 2014.
- [9] N. Krombach, D. Droschel, and S. Behnke, Evaluation of stereo algorithms for obstacle detection with fisheye lenses, Proc. of ISPRS Annals of the Photogrammetry, Remote Sensing and Spatial Information Sciences, Volume II-1/W1, 2015
- [10] P. Furgale *et al.*, Toward automated driving in cities using close-to-market sensors: An overview of the V-Charge Project, Proc. of IEEE Intelligent Vehicles Symposium (IV), 2013.
- [11] S. K. Gehrig, Large-field-of-view stereo for automotive applications, Proc. of OmniVis, Vol. 1, 2005.
- [12] D. Kim, J. Choi, H. Yoo, U. Yang, and K. Sohn, Rear obstacle detection system with fisheye stereo camera using HCT, Journal of Expert Systems With Applications, vol. 42, no. 17, pp. 6295-6305, Oct. 2015.
- [13] M. Ruffi, D. Scaramuzza, and R. Siegwart, Automatic detection of checkerboards on blurred and distorted images, Proc. of the IEEE/RSJ International Conference on Intelligent Robots and Systems (IROS 2008), pp. 3121-3126, Nice, France, September 2008.
- [14] P. F. Alcantarilla, J. Nuevo and A. Bartoli, Fast explicit diffusion for accelerated features in nonlinear scale spaces, Proc. of British Machine Vision Conference (BMVC), Bristol, UK, September 2013.
- [15] P. F. Alcantarilla, A. Bartoli and A. J. Davison, KAZE Features, Proc. of European Conference on Computer Vision (ECCV), The series Lecture Notes in Computer Science, Vol. 7577, pp. 214-227, Firenze, Italy, October 2012.